

## DURABILITY OF THE MULTICOMPONENT NITRIDE COATINGS BASED ON TiN AND (Ti, Al)N DEPOSITED BY PIII&D METHOD

V.V. Vasyliiev\*, V.S. Goltvyanytsya\*\*, S.K. Goltvyanytsya\*\*, A.A. Luchaninov\*,  
V.G. Marinin\*, E.N. Reshetnyak\*, V.E. Strel'nitskij\*, G.N. Tolmachova\*  
\*National Science Center "Kharkov Institute of Physics and Technology",  
Kharkov, Ukraine;  
\*\*Real Ltd., Ukraine

The multicomponent nitride coatings based on TiN and (Ti, Al)N with small additions of Y, Re, Ni, Cr, Si, Mo, Fe synthesized by the PIII&D method from the filtered cathodic-arc plasma. The crystalline nitride phase in all coatings is of the cubic structure of NaCl type. All investigated coatings were characterized with the hardness of 23...36 GPa and Young's modulus of 324...436 GPa. The addition of dopants reduces the average rate of cavitation and abrasive wear of the coatings. The best durability demonstrated coating deposited from the cathode of the  $Ti_{0.49}Al_{0.50}Y_{0.006}Re_{0.0005}$  composition. This coating also demonstrated high thermal stability.

### INTRODUCTION

Doping the nitride coatings with small amounts of B, Si, Cr, V, Nb, Y, Hf and other elements that are traditionally added to the heat-resistant alloys can significantly improve their wear and heat resistance [1–14]. It enables to develop new multicomponent nanostructured coatings used for protection the tools and machine components that undergo extreme environmental conditions.

The PIII&D (plasma immersion ion implantation and deposition) method combined with FVAD (filtered vacuum arc deposition) is powerful tool for fabricating the wide range of high quality coatings [15]. Among the factors which affect the mechanical and functional properties of the nitride coatings the chemical composition and energy of ions deposited (adjusted by the substrate potential) were examined. However, other deposition process parameters should be taken into consideration too, for example, plasma gas composition (or the partial pressure of nitrogen and argon) also plays an important role [16–19]: nitrogen ( $N_2$ ) being the reactive gas for nitride synthesis and argon (Ar) gas is widely used for improving operation stability of the vacuum-arc sources.

Present work is a logical continuation of our earlier investigations [20, 21], where the structure and properties of the TiN, (Ti, Al)N and (Ti, Al)N coatings doped with Y were studied. We use the developed method of the nitride coatings deposition for search new perspective coatings of novel elemental compositions. Furthermore in the present experiments Ar pressure was varied as an important parameter of the technological deposition process, because different cathode materials need different Ar pressure values for supplying stable vacuum arc source operation as it follows from the experiment.

The main goal of the present work was development novel multicomponent nitride coatings by PIII&D method using filtered vacuum-arc plasma source and as-cast Ti-based and TiAl-based cathodes with additions of Cr, Si, Y, Re, Ni, Mo, Fe in various combinations and comparative estimation of their functional properties. The influence of doping elements and deposition

process parameters on the composition, structure, mechanical characteristics and functional properties of the multicomponent nitride coatings was investigated. We tested the doped coatings on the cavitation and abrasion resistance as well as their oxidation resistance.

### 1. EXPERIMENTAL METHODS

The nitride coatings of Ti-N and Ti-Al-N systems doped with small additions of Cr, Si, Y, Re, Ni, Mo, Fe were produced by vacuum-arc method. The straight magnetoelectric filter was used for removing the macroparticles from the plasma stream [22]. The scheme of the installation used for coatings deposition was presented elsewhere [20]. The alloys of  $Ti_{0.49}Al_{0.50}Y_{0.01}$ ,  $Ti_{0.86}Si_{0.13}Y_{0.01}$ ,  $Ti_{0.48}Al_{0.50}Ni_{0.01}Cr_{0.01}$ ,  $Ti_{0.88}Mo_{0.11}Fe_{0.01}Y_{0.002}$ ,  $Ti_{0.49}Al_{0.50}Y_{0.006}Re_{0.0005}$ ,  $Ti_{0.49}Al_{0.50}Y_{0.01}Re_{0.001}$  elemental composition produced via vacuum-arc remelting in argon atmosphere (by Real Ltd., Zaporozhye, Ukraine) were used as cathode materials in vacuum-arc plasma source. The coatings with the thickness in the range of 6...8  $\mu m$  were deposited on stainless steel substrates with geometry 17×20×0.6 mm. The distance from the filter outlet to the specimens was of 180 mm. A glow discharge in argon at pressure of  $P_{Ar} = 4$  Pa and pulsed substrate bias potential of 2.5 kV amplitude relative to the vacuum chamber was used for cleaning the substrates surface. Coatings were deposited at an arc current of 100 A. Partial nitrogen and argon pressure in the vacuum chamber were in the ranges 0.1...0.2 and 0.01...0.02 Pa accordingly. The pulsed potential of negative polarity with the amplitude of 1.5...2.5 kV, pulse duration 5  $\mu s$  and repetition frequency 24 kHz was applied to the substrate. In the time intervals between the pulses the substrate was at "floating" potential of 3...15 V. Additional magnetic focusing of the plasma flow in the vacuum chamber ensured a high deposition rate of 12...16  $\mu m/h$ . Coating deposition duration was 30 min.

The elemental composition of the coatings was measured by X-ray fluorescence analysis (XRA) with the vacuum scanning crystal diffraction spectrometer SPRUT. The concentration of Ti, Al and doping elements was calculated without taking into account the nitrogen content. It is well known that in some cases,

when the characteristic lines intensity depends on the thickness of thin film, the values of the elements concentration determined by the XRA spectrometer requires correction for the thickness [23]. In the present experiments correction on the coating thickness was applied only for measurements concentrations in the coatings which contained Y, Re and Mo elements.

The X-ray diffraction (XRD) measurements were performed on a DRON-3 diffractometer in the filtered Cu-K $\alpha$  radiation on ( $\theta$ -2 $\theta$ ) configuration. Judging by the position of the nitride diffraction lines of a cubic NaCl-type structure the value of the crystal lattice parameter in the direction of the normal to the film surface was determined. The size of the crystal grains (coherent scattering zone) of nitride films was calculated using the Scherrer relation, in which the full width at half maximum (FWHM) was taken from the (111) or (220) peaks in XRD patterns.

The hardness ( $H$ ) and reduced Young's modulus ( $E$ ) of the coatings was measured with a G200 nanoindenter in CSM (continuous stiffness measurement) mode. The  $H$  and  $E$  values were taken at the depth of indentation, equal to 10% of the film thickness.

The erosion under the action of cavitation in distilled water at room temperature was studied in the facility with an ultrasonic vibrator [21]. The mass loss was measured with an accuracy of 0.015 mg. As a rule the tests lasted until visually watched open-ended pores in the coating began to form, but for all of these the depth of erosive defects did not reach 5...6  $\mu\text{m}$ . Owing to such restriction only the coating material loss was measured in the test, not the substrate one. The average wear rate was used as a criterion for the coating durability.

The abrasive wear of the coatings was determined by the gravimetric method using the scheme "plane specimen – rotating abrasive disk" at linear velocity of 4.38 m/s and normal load of 2.2 N. The test duration

was 40 min. Coatings adhesion was evaluated on the results of the Rockwell indenter test.

The oxidation resistance of the coatings was studied with a thermal analyzer (Netzsch STA 449 F Jupiter) in the range of 20...1000  $^{\circ}\text{C}$  at a heating rate of 20 K/min in a mixture of dry nitrogen (80 vol.%) and oxygen (20 vol.%) with a flow rate of 70 ml/min.

## 2. RESULTS AND DISCUSSION

### 2.1. STRUCTURE AND PROPERTIES OF THE MULTICOMPONENT TiN-BASED AND (Ti, Al)N-BASED NITRIDE COATINGS DOPED WITH Cr, Si, Y, Ni, Mo, Fe

The coatings described in this section were deposited under identical process parameters: nitrogen partial pressure 0.1 Pa, argon partial pressure 0.01 Pa, the substrate bias potential amplitude of 1.5 kV [20]. The cathodes compositions and characteristics of the multicomponent nitride coatings are listed in Table 1. For comparison the characteristics of the TiN and (Ti $_{0.5}$ Al $_{0.5}$ )N coatings deposited at the same process parameters are shown too. On the results of XRA measurements the concentration of the doping elements in the coatings approximately equals to that in the cathode materials. The only exception is Si concentration in the coating of the specimen #2 which is three times lower than that in the cathode material. Such effect was reported too by the authors of the works [24, 25].

The X-ray diffraction patterns of the multicomponent nitride coatings are shown in Fig. 1. It was revealed the only crystalline nitride phase in the films, namely a cubic NaCl-type structure. The only exception is the specimen #3 (the coating deposited using the Ti $_{0.88}$ Mo $_{0.11}$ Fe $_{0.01}$ Y $_{0.002}$  cathode), which included another phase, probably Mo $_9$ Ti $_4$ . Two phases were also revealed in vacuum-arc nitride coatings of Mo-N system deposited at high substrate bias [26].

Table 1

The results of the XRD analysis and mechanical properties of the multicomponent nitride coatings produced with use of the cathodes of various composition (amplitude of pulse substrate bias potential 1.5 kV; partial pressure of the gas mixture: nitrogen – 0.1 Pa and argon – 0.01 Pa)

Specimen #	Composition of the cathode used for coating deposition, at. %	Coatings characteristics					
		Nitride lattice period, nm	Grain size, nm	Preferred orientation	Integral intensity of the nitride lines, a.u.	H, GPa	E, GPa
1	Ti	0.4279	13	(hh0)	2760	29.5	404
2	Ti $_{0.86}$ Si $_{0.13}$ Y $_{0.01}$	0.4283	8	(hh0)	1900	32.1	387
3	Ti $_{0.88}$ Mo $_{0.11}$ Fe $_{0.01}$ Y $_{0.002}$	0.4296	6	(hh0)	1078	28.5	374
4	Ti $_{0.5}$ Al $_{0.50}$	0.4212	7	(hh0)	1702	31.4	436
5	Ti $_{0.48}$ Al $_{0.50}$ Ni $_{0.01}$ Cr $_{0.01}$	0.4208	6	(hh0)	370	25.8	324
6	Ti $_{0.49}$ Al $_{0.50}$ Y $_{0.01}$	0.4209	9	(hh0)	6160	35.8	418

Table 2

Deposition parameters and characteristics of the coatings deposited with use of  $Ti_{0.49}Al_{0.50}Y_{0.01}$  cathode

Specimen #	Amplitude of pulses U, kV	Partial gas pressure, Pa		Coating composition, at% metal sub-lattice	Preferred orientation	Integral intensity of the nitride lines, a.u.	H, GPa	E, GPa	Abrasive wear rate, $10^{-4}$ mg/min	Cavitation tests	
		N <sub>2</sub>	Ar							Duration of through defect formation, h	Wear rate, $10^{-3}$ mg/h
7	2.5	0.1	0.01	$Ti_{0.51}Al_{0.48}Y_{0.01}N$	(hh0)	2184	30.1	380	12.5	12	2.7
8	2.5	0.1	0.015	$Ti_{0.51}Al_{0.48}Y_{0.01}N$	(h00)	1400	27.5	364			
9	2.5	0.1	0.018	$Ti_{0.54}Al_{0.41}Y_{0.01}N$	(hhh)	630	32.5	378	1.7	8	7.6
10	2.5	0.2	0.018	$Ti_{0.52}Al_{0.47}Y_{0.01}N$	(h00)	850	22.9	325	1.7	8	2.9
6	1.5	0.1	0.01	$Ti_{0.49}Al_{0.50}Y_{0.01}N$	(hh0)	6160	35.8	418	3.7	12	3.8
11	1.5	0.1	0.015	$Ti_{0.54}Al_{0.45}Y_{0.01}N$	(hhh)	270	30.1	360	5.0	4	9.7
12	1.5	0.2	0.018	$Ti_{0.52}Al_{0.47}Y_{0.01}N$	(h00)	900	31.1	383	3.3	4	2.0

The nitride phase in all coatings has a strong texture with a preferred orientation of the (hh0) crystallographic planes parallel to the surface of the coating. The (220) peak is dominant in all XRD patterns, but its intensity for different coatings differs greatly. At the same time width of the (220) peak is close enough for all coatings. This fact indicates that the grain size of crystallites in all coatings is nearly of the same value which does not exceed 13 nm (see Table 1).

For the films fabricated from the cathodes based on  $Ti_{0.5}Al_{0.5}$  alloy with different dopants (specimens #4–6), a nitride crystal lattice period amounts to about 0.421 nm. This value is considerably lower than that for the films deposited from the cathodes based on Ti with dopants (specimens #1–3): 0.428...0.430 nm. All investigated coatings were characterized by hardness of 26...36 GPa and Young's modulus of 324...436 GPa.

Hardness of the  $Ti_{0.97}Si_{0.03}Y_{0.02}N$  coating was 32.1 GPa, that is slightly higher than that of the TiN one (specimen #1) produced using the same process parameters. This result agrees well with the well known fact of increase in hardness of the TiN coating in case Si doping [24]. On the contrary, addition of  $Mo_{0.08}Fe_{0.01}Y_{0.005}$  resulted in decrease in hardness of the coating to 28.5 GPa. The  $Ti_{0.49}Al_{0.47}Ni_{0.03}Cr_{0.01}N$  coating was characterized by lower hardness (25.8 GPa) than the  $Ti_{0.5}Al_{0.5}N$  one (31.4 GPa).

The results of cavitation tests of specimens with the coatings of various compositions are presented in Fig. 2. The dependencies of the mass losses show that all investigated coatings are characterized by low cavitation wear, much lower than that of the substrate (austenite stainless steel). Fig. 3 shows the micrographs of the surface of the coatings after the test.

It can be seen that the TiN coating has the worst cavitation resistance. Few pits are observed on its surface which reach the substrate during the first 1.5 h period of the test because of strongly pronounced columnar structure of the coating [21].

The nitride coatings with additions of Ni, Cr, Si, Mo, Fe show better cavitation resistance than TiN one. They withstood cavitation impact for 2, 3 h before the wear rate began increased sharply. A sufficiently large number of defects in form of small pits and cracks on the surface of these coatings are visible after all cavitation tests (see Fig. 3,b). The  $Ti_{0.5}Al_{0.5}N$  coating, doped with Y, demonstrated the best cavitation resistance. It stood the 12 hours testing. The wear rate of this coating was lower than that of the rest, and the number of defects on the eroded surface was little (see Fig. 3,c). This coating is also characterized by the highest hardness of about 36 GPa. The results of abrasive wear tests of coatings are shown in Fig. 4. The abrasive wear rate of the doped coatings does not exceed  $7 \cdot 10^{-3}$  mg/min. It is three orders of magnitude lower than that of uncoated stainless steel and an order of magnitude lower than the wear rate of the TiN coating. The TiN coatings doped with Mo, Fe (specimen #3) and the (Ti, Al)N coatings doped with Y (specimen #6) were the most abrasion resistant. Thus, the coatings fabricated from  $Ti_{0.49}Al_{0.50}Y_{0.01}$  cathode have good promise as resistant material against both types of wear.

The search for correlations between the cavitation erosion resistance and properties of materials remains up to now the issue of great importance [27–30]. Our observations did not reveal correlation between the cavitation erosion resistance and hardness of multicomponent nitride coatings. However, the experiment shows clearly that the addition of impurities improves durability. This may be due to suppression the columnar structure in coating during its growth because of the doping [4, 21].

An important characteristic of the coatings is also the quality of the adhesion to the substrate. We used the Rockwell indenter test for evaluation the adhesion level. In Fig. 5 the photographs of the indenter prints on the coating surface after testing are presented.

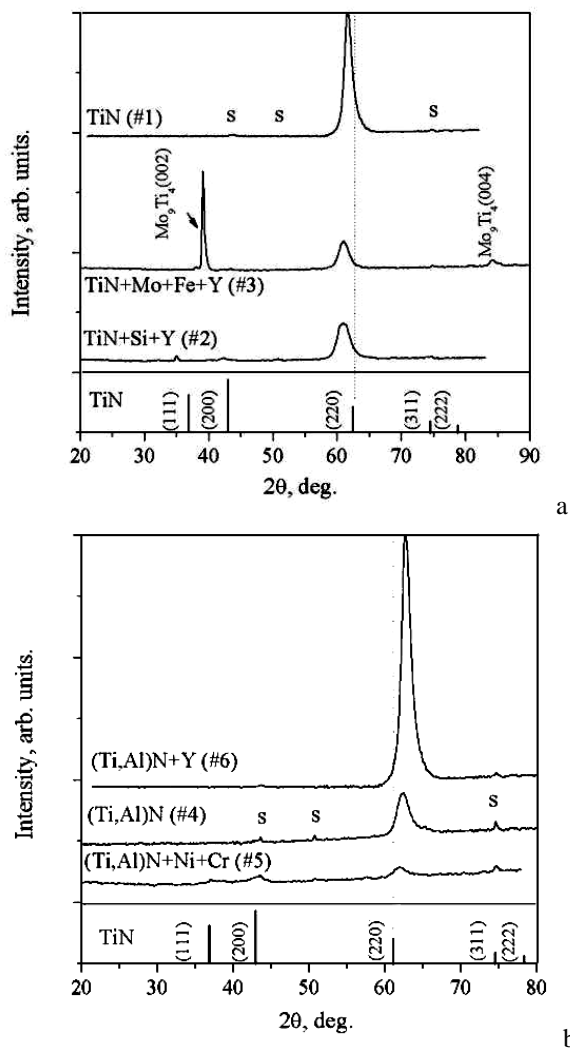


Fig. 1. XRD scans of the nitride coatings, deposited using the cathodes of different elemental composition (amplitude of pulse substrate bias potential 1.5 kV; partial pressure of the gas mixture:  $N_2 - 0.1$  Pa and Ar - 0.01 Pa):  
 a - Ti-based cathodes;  
 b -  $Ti_{0.5}Al_{0.5}$ -based cathodes

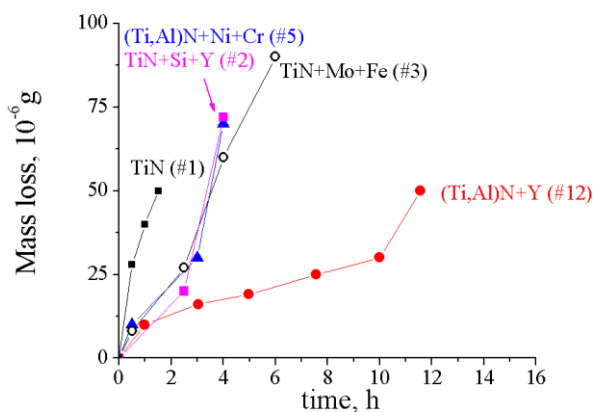
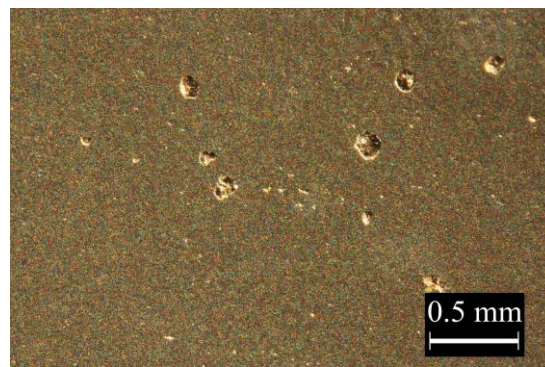
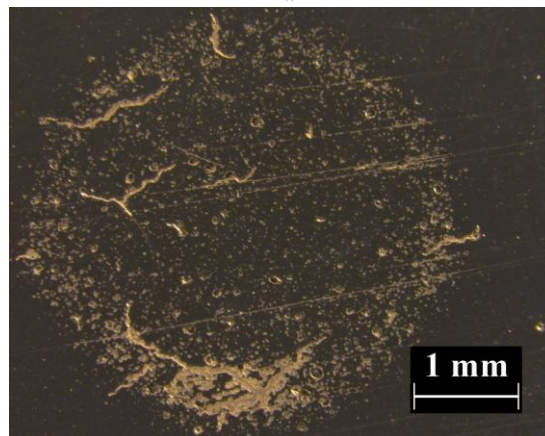


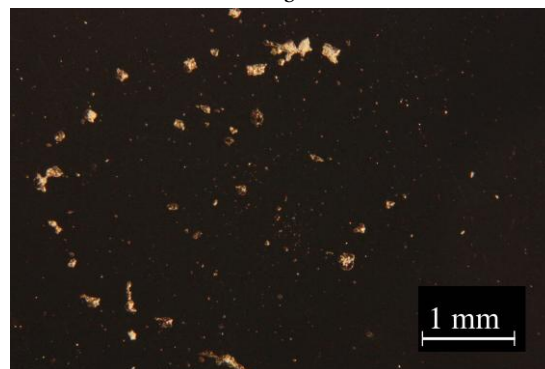
Fig. 2. Kinetic curves of the cavitation wear of the TiN-based and (Ti, Al)N-based coatings doped with the different elements (amplitude of pulse substrate bias potential 1.5 kV; partial pressure of the gas mixture:  $N_2 - 0.1$  Pa and Ar - 0.01 Pa)



a



b



c

Fig. 3. Surface images of the TiN-based and (Ti, Al)N-based coatings doped with different elements after cavitation test (amplitude of pulse substrate bias potential 1.5 kV; partial pressure of the gas mixture:  $N_2 - 0.1$  Pa and Ar - 0.01 Pa): a - TiN; b - TiN+Si+Y (specimen #2); c - (Ti,Al)N+Y (specimen #6)

There is an evident difference in adhesion levels of the TiN-based and (Ti, Al)N-based coatings. Delamination of the TiN+Si+Y and TiN+Mo+Fe+Y coatings in their contact with the Rockwell indenter indicates poor adhesion of these coatings to the substrate. On the contrary, the (Ti, Al)N+Ni+Cr and (Ti, Al)N+Y coatings do not break down and not peel off from the substrate showing a fairly good adhesion. There are no radial cracks at the edges of the prints on the surface of these coatings. So, the best mechanical characteristics along with good adhesion and durability demonstrated the (Ti, Al)N+Y coating. The results of detailed investigations of the coatings of this system are presented in the next section.

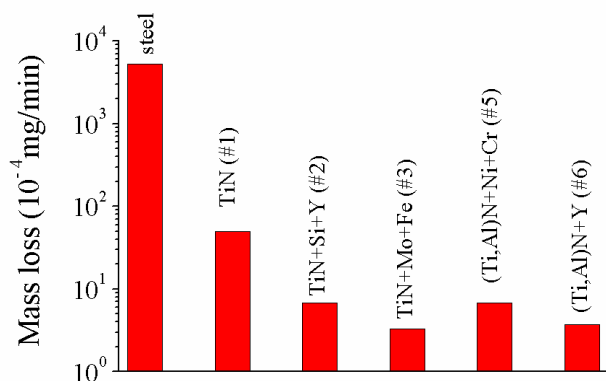


Fig. 4. Abrasive wear rate of the TiN-based and (Ti, Al)N-based coatings doped with different elements (amplitude of pulse substrate bias potential 1.5 kV; partial pressure of the gas mixture:  $N_2 - 0.1$  Pa and Ar – 0.01 Pa)

## 2.2. INFLUENCE OF THE DEPOSITION PARAMETERS ON THE STRUCTURE AND WEAR RESISTANCE OF THE (Ti, Al)N COATINGS DOPED WITH Y

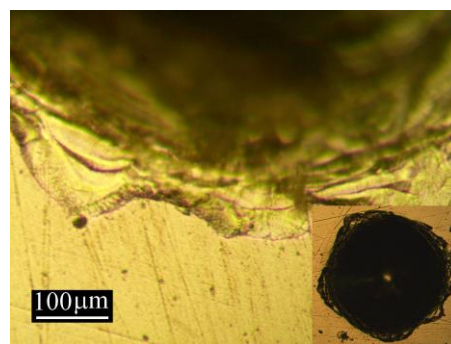
This section presents the results of studies of the effect of the partial pressure of gases (nitrogen, argon) and the amplitude of the high-voltage pulsed bias potential on the characteristics of the coatings produced using the  $Ti_{0.49}Al_{0.50}Y_{0.01}$  cathode. Table 2 shows the deposition parameters, structural and mechanical characteristics of the coatings and the results of cavitation and abrasion tests.

Cubic solid solution is the sole nitride phase, which is detected by X-ray analysis in the studied (Ti,Al)N coatings doped with Y. However, it should be noted that some of the coatings may have an amorphous-crystalline (heterophasic) structure, i. e. contain a substantial amount of amorphous phase. This is evidenced by the extremely low intensity of the reflections in its XRD patterns. Thus the width of the diffraction peaks is not very different. The grain size of such nitride coatings is in the range of 6...8 nm.

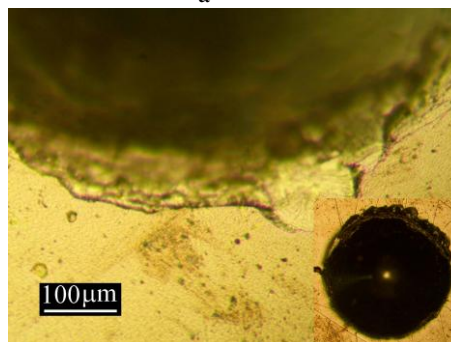
It is well known that the integrated intensity of the diffraction lines of the crystalline phase is proportional to its content in the irradiated volume [31]. It is decreased greatly with increase in Ar content in gas mixture (see Table 2). At the same time the changes of the preferred orientation of nitride grains occur.

Quantitative description of the texture was done by calculations of the texture coefficients for reflections (111), (200) and (220). The texture coefficient was defined in accordance with [32].

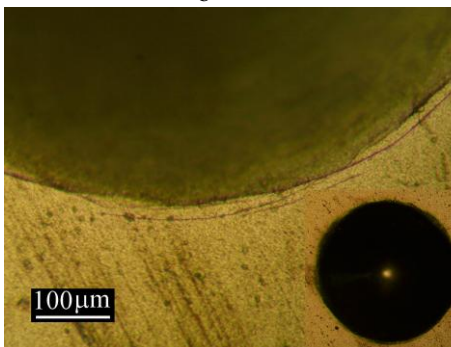
Dependence of the texture coefficient on argon partial pressure for specimens #7–9 deposited at pulsed bias potential amplitude of 2.5 kV and nitrogen partial pressure of 0.1 Pa is shown in Fig. 6. With increase in argon pressure in the range of 0.01...0.018 Pa the change in the preferred orientation of the crystallites in the coatings occurs in the following sequence: (hh0)→(h00)→(hhh). The preferential grain orientation in the other investigated nitride coatings shown in Table 2.



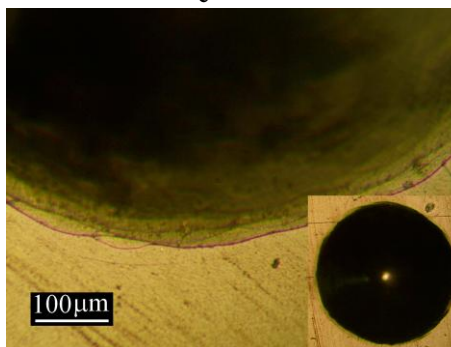
a



b



c



d

Fig. 5. Fragments of the Rockwell imprints on the surface of TiN-based and (Ti, Al)N-based coatings doped with the different elements: a – TiN+Si+Y; b – TiN+Mo+Fe+Y; c – (Ti,Al)N+Ni+Cr; d – (Ti, Al)N+Y. Insertions are the common view of the imprints

It can be seen that for coatings deposited at a lower bias potential of 1.5 kV (specimens #6, 11) such change in orientation from (hh0) to (hhh) is observed at a lower argon pressure – 0.015 Pa. Thus, with increase in the argon partial pressure the crystal structure of the nitride coatings is changed from crystalline to an amorphous-crystalline heterophasic one and preferred orientation from (hh0) to (hhh). Changing the preferred orientation

of the grains in the vacuum arc nitride coatings as a result of adding argon to the gas phase was also observed by the authors of [18, 33].

It is well known that the ion bombardment significantly affects the microstructure of films growing from the vapor phase [34]. In general, two main effects occur by increasing the argon ion bombardment during deposition. (1) A rapid increase in the number of secondary nuclei and discontinuance of columnar growth. (2) Increase in strain energy of the film due to increase in energy of arrival ions and its sub-implantation. In our case, influence of the ions bombardment becomes stronger at higher argon partial pressure and higher substrate bias voltage.

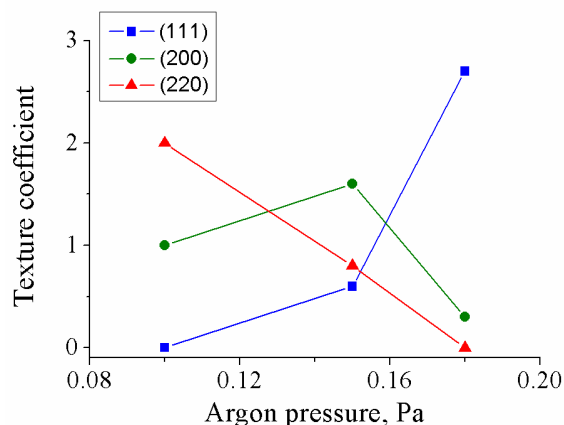


Fig. 6. Effect of the partial pressure of Ar on texture coefficients of the coatings obtained using the  $Ti_{0.49}Al_{0.50}Y_{0.01}$  cathode (amplitude of pulse substrate bias potential 2.5 kV, partial pressure of  $N_2$  in the gas mixture of 0.1 Pa)

The texture evolution of a film was predicted by the authors of the work [18] in frames of minimization the overall energy of the film, which includes the surface free energy, interface energy and strain energy. When the films were grown under low-stress conditions (low argon pressure and bias potential), the strain energy should not dominate the overall energy of the films, and (100) or (110) orientations would be the preferred these because they possess the lowest surface energy compared to the (111) one for the TiN films. Vice versa, when the films were grown under the high stress, the strain energy determines the overall energy of the films, the (111) orientation became preferred one because it has the lowest strain energy [35].

Our studies have shown that if a high voltage pulse bias potential is applied to a substrate, the wear resistance of vacuum-arc deposited nitride coatings depends greatly on the argon content in  $N_2+Ar$  gas mixture because of the structural changes caused in the coating by argon ion bombardment. Thus, increase in argon content in the gas mixture significantly deteriorates the cavitation resistance of the deposited coatings (see Table 2).

Fig. 3,c represents typical for all the coatings image of eroded surface with some small enough pits. The observed average wear rate correlates with the cavitation defects density. The results indicate that the coatings obtained at elevated partial pressure of argon are characterized with both enhanced density of erosion

defects on the surface and increased speed of deepening the erosion pits under the cavitation impact.

To explain these results it should be noted that an important factor which determines the crystalline structure and properties of the coatings is their elemental composition, which can be varied to some extent by changing parameters of the deposition process. The XRA data on the ratio of the metal components in the coating which are presented in Table 2 show that with increasing partial pressure of argon the content of aluminum in the coating is reduced. This may be due to selective sputtering of light elements atoms from the surface under argon ion bombardment during the deposition of the coatings [19]. With increase in argon pressure the intensity of bombardment is increased, and the concentration of aluminum in the coating decreased. All of the above can be fully attributed to the lightest coating component – nitrogen.

It is very likely that the amorphous-crystalline structure in the coatings deposited at higher partial pressure of argon (specimens #9, 11) arises in consequence of deviation from stoichiometric nitride composition. XRD data on the structure of the coatings deposited at increased to 0.2 Pa nitrogen partial pressure (specimens #10, 12) confirm this assumption. More nitrogen in the gas mixture promotes formation of more crystalline nitride phase and stoichiometric composition. Indeed, in these coatings the aluminum concentration is of 47% and the degree of crystallinity is increased, and the preferred orientation (h00) returns. As a result, cavitation resistance of the coating is improved.

Concerning the abrasion resistance, all coatings are characterized by rather low values of the abrasive wear rate. However, low abrasive wear does not guarantee high cavitation resistance of the coating (specimens #9, 10). There was not observed unambiguous correlation between the hardness and wear resistance of the coatings. The rates of cavitation and abrasive wear of the specimen #6 with hardness value of 36 GPa are higher than these of the specimen #10 with hardness value of 23 GPa. These results are in line with the findings of our previous work [21], where it was shown that the cavitation and abrasive wear resistance of coatings was determined by a complex variety of factors including hardness, crystallite size and its preferred orientation, surface roughness and residual stress level.

### 2.3. PROPERTIES OF THE (Ti, Al)N-BASED COATINGS SIMULTANEOUSLY DOPED WITH Y AND RE

The (Ti, Al)N coatings simultaneously doped with Y and Re, whose characteristics are given in Table 3, show the same basic structural features and properties as the (Ti, Al)N coating doped with Y alone. Increase in partial pressure of argon during deposition leads to a reduction in the aluminum content in the coating, alteration structure from the predominantly crystalline onto the amorphous-crystalline one and deterioration of their durability. Specimen #13 (cathode composition  $Ti_{0.49}Al_{0.50}Y_{0.006}Re_{0.0005}$ ) demonstrated the best resistance against cavitation and abrasive wear among all specimens investigated in our experiments. Fig. 7 illustrates the effect of doping with Y and Re on the

cavitation wear of the (Ti, Al)N coatings, deposited under optimum gas mixture parameters (nitrogen and argon partial pressure of 0.1 and 0.01 Pa accordingly). For the (Ti, Al)N coating, simultaneously doped with Y

and Re, formation of open-ended defects under cavitation lasts 14 h, and the rate of cavitation wear is reduced noticeably.

Table 3

Deposition parameters and characteristics of (Ti,Al)N coatings, doped with Y and Re

Specimen #	Amplitude of pulses U, kV	Partial gas pressure, Pa		Coating composition, at.% metal sub-lattice	Preferred orientation	Integral intensity of the nitride lines, a.u.	H, GPa	E, GPa	Rate of abrasive wear, $10^{-4}$ mg/min	Cavitation tests	
		N <sub>2</sub>	Ar							Duration of through defect formation, h	Wear rate, $10^{-3}$ mg/h
13	1.5	0.1	0.01	Ti <sub>0.53</sub> Al <sub>0.46</sub> Y <sub>0.006</sub> Re <sub>0.0005</sub> N	(h00)	1000	28.2	354	1.7	14	2.0
14	1.5	0.1	0.016	Ti <sub>0.53</sub> Al <sub>0.46</sub> Y <sub>0.01</sub> Re <sub>0.001</sub> N	(hhh)	252	29.4	341	5	8	13.8
15	2.5	0.1	0.016	Ti <sub>0.57</sub> Al <sub>0.42</sub> Y <sub>0.01</sub> Re <sub>0.001</sub> N	(hhh)	510	29.4	355	1.7	10	4.1

As for amorphous-crystalline coatings deposited at a higher partial pressure of argon (specimens #14, 15) using the Ti<sub>0.49</sub>Al<sub>0.50</sub>Y<sub>0.01</sub>Re<sub>0.001</sub> cathode, their cavitation resistance is substantially lower than that for the specimen #13 with predominantly crystalline structure. At that, hardness and Young's modulus of these coatings are close within the measurement error.

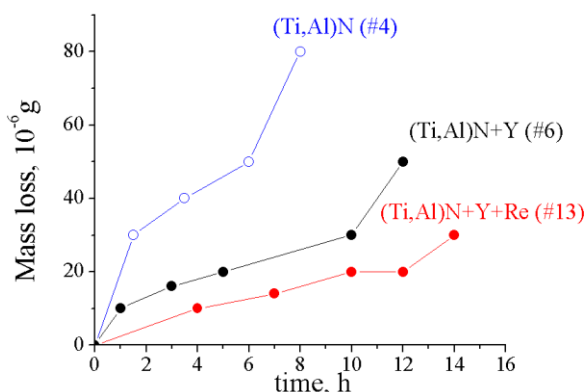


Fig. 7. Effect of doping the (Ti, Al)N coating with Y and Re on the kinetic curves of cavitation wear (amplitude of pulse substrate bias potential 1.5 kV, partial pressure of the gas mixture: N<sub>2</sub> – 0.1 Pa and Ar – 0.01 Pa)

Another important characteristic for technical applications of the coatings is their resistance to oxidation. Fig. 8 shows the thermogravimetric curves of the specimens with the (Ti, Al)N coatings doped with Y and Re. It can be seen that adding any of used additions to the base elemental composition (Ti, Al)N improves the oxidation resistance, but to a variable degree. The thermal stability of the specimen #13, which showed the best wear resistance, is also maximal. Its oxidation onset temperature is 950 °C and the weight gain at 1000 °C is minimal (0.01%). These characteristics are close to the values obtained previously for the Ti<sub>0.49</sub>Al<sub>0.50</sub>Y<sub>0.01</sub>N coating [20]. Specimen #14, synthesized at a higher partial pressure of argon, begins to oxidize slightly earlier, that is at 810 °C, but after some time the

oxidation rate is decreased dramatically, and its mass gain at 1000 °C substantially coincides with that for the specimen #13.

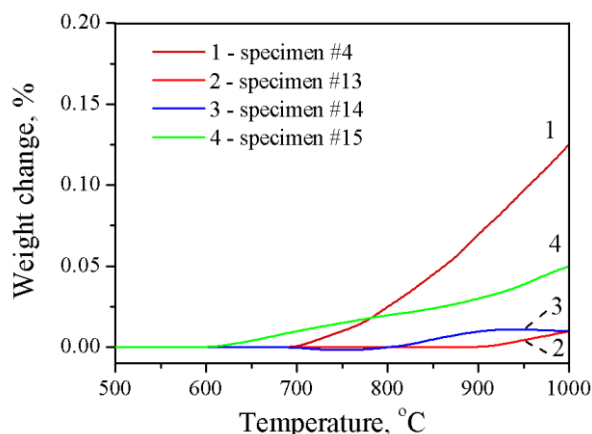


Fig. 8. Thermogravimetric curves of specimens with the (Ti, Al)N coating and these, doped with Y and Re, deposited at partial pressure of N<sub>2</sub> in the gas mixture of 0.1 Pa and various values of pulsed substrate bias potential amplitude and argon partial pressure: 1 – (Ti, Al)N (amplitude of 1.5 kV, Ar pressure of 0.01 Pa); 2 – (Ti, Al)N+Y+Re (amplitude of 1.5 kV, Ar pressure of 0.01 Pa); 3 – (Ti, Al)N+Y+Re (amplitude of 1.5 kV, Ar pressure of 0.016 Pa); 4 – (Ti, Al)N+Y+Re (amplitude of 2.5 kV, Ar pressure of 0.016 Pa)

Apparently, an oxide film is formed on a specimen surface and therefore prevents further intensive oxidation. Also, it can be seen that increase in the substrate bias potential during deposition leads to the deterioration of the oxidation resistance. Specimen #15, deposited at pulsed bias potential with amplitude of 2.5 kV, begins to oxidize even before the (Ti, Al)N coating, at a temperature of 625 °C, however, its oxidation rate is 2.5 times lower. Thus, specimen #13 showed all-time high durability against various deleterious factors simultaneously: thermal oxidation,

abrasive and cavitation wear. The role of yttrium and rhenium additions is still largely unclear, but the results of the tests show promising possibilities in improving the protective properties of the multicomponent nitrides deposited by the PIII&D method.

## CONCLUSIONS

The structure and properties of the multicomponent TiN and (Ti, Al)N coatings with small additions of Y, Re, Ni, Cr, Si, Mo, Fe, synthesized by the PIII&D method from the filtered cathodic arc plasma were investigated. It was established that crystalline nitride phase in all coatings is of the cubic structure of the NaCl type, but its quantity and the preferred orientation of the crystallites depends on the elemental composition of the gas phase and the amplitude of the high voltage pulsed substrate bias potential. All investigated coatings were characterized by relatively high hardness of 23...36 GPa and Young's modulus of 324...436 GPa.

The cavitation and abrasion wear resistance of the nitride multicomponent TiN-based and (Ti, Al)N-based coatings were investigated. The addition of dopants reduced the average rate of both types of wear. The most efficient was the doping of the (Ti, Al)N coatings with small amounts of Y and Re. The best durability demonstrated coating produced using the cathode  $Ti_{0.49}Al_{0.50}Y_{0.006}Re_{0.0005}$ , at pulsed substrate bias potential amplitude of 1.5 kV and partial pressure of nitrogen of 0.1 Pa and argon of 0.01 Pa. This coating demonstrated high thermal stability, as well.

It was found that the structure and mechanical properties of the coatings are very sensitive to the parameters of the deposition process. Increase in the partial pressure of argon in the range of 0.01...0.018 Pa and pulsed substrate bias potential amplitude from 1.5 to 2.5 kV during deposition of the (Ti, Al)N coatings doped with Y and Re results in formation the amorphous-crystalline structure with less amount of crystalline phase, characterized by significantly worse cavitation and oxidation resistance. Both cavitation and abrasive resistance of the amorphous-crystalline coatings with (hhh) orientation are significantly worse than that of predominantly crystalline coatings with (hh0) or (h00) orientation.

Thus, the multicomponent nitride coatings with close elemental composition and mechanical properties can fundamentally differ in their durability and thermal oxidation resistance because of the peculiarities of its crystal structure.

## REFERENCES

1. L. Hultman. Thermal stability of nitride thin films // *Vacuum*. 2000, v. 57, p. 1-30.
2. V.H. Derflinger, A. Schutze, M. Ante. Mechanical and structural properties of various alloyed TiAlN-based hard coatings // *Surf. Coat. Technol.* 2006, v. 200, p. 4693-4700.
3. L. Rebouta, F. Vaz, M. Andritschky, M.F. da Silva. Oxidation resistance of (Ti, Al, Zr, Si)N coatings in air // *Surf. Coat. Technol.* 1995, v. 76-77, p. 70-74.
4. S. PalDey, S.C. Deevi. Single layer and multilayer wear resistant coatings of (Ti, Al)N: a review // *Materials Sci. Eng.* 2003, v. A342, p. 58-79.
5. M. Pfeiler, K. Kutschej, M. Penoy, C. Michotte, C. Mitterer, M. Kathrein. The effect of increasing V content on structure, mechanical and tribological properties of arc evaporated Ti-Al-V-N coatings // *Int. Jour. of Refractory Metals*. 2009, v. 27, p. 502-506.
6. S.K. Kim, P.V. Vinh, J.H. Kim, T. Ngoc. Deposition of superhard TiAlSiN thin films by cathodic arc plasma deposition // *Surf. Coat. Technol.* 2005, v. 200, p. 1391-1394.
7. K. Yamamoto, S. Kujime, G. Fox-Rabinovich. Effect of alloying element (Si,Y) on properties of AIP deposited (Ti,Cr,Al)N coating // *Surf. Coat. Technol.* 2008, v. 203, p. 579-583.
8. S.Q. Wang, Li Chen, B. Yang, K.K. Chang, Yong Du, Jia Li, Tie Gang. Effect of Si addition on microstructure and mechanical properties of Ti-Al-N coating // *Int. Jour of Refr. Metals*. 2010, v. 28, p. 593-596.
9. M. Moser and P.H. Mayrhofer. Yttrium-induced structural changes in sputtered  $Ti_{1-x}Al_xN$  thin films // *Scripta Materialia*. 2007, v. 57, p. 357-360.
10. R. Rachbauer, A. Blutmager, D. Holec, P.H. Mayrhofer. Effect of Hf on structure and age hardening of Ti-Al-N thin films // *Surf. Coat. Technol.* 2012, v. 206, p. 2667-2672.
11. H. Riedl, D.Holec, R. Rachbauer, P. Polcik, R. Hollerweger, J. Paulitsch, Paul H. Mayrhofer. Phase stability, mechanical properties and thermal stability of Y alloyed Ti-Al-N coatings // *Surf. Coat. Technol.* 2013, v. 235, p. 174-180.
12. E. Pfluger, A. Schroer, P. Voumard, L. Donohue, W.-D. Munz. Influence of incorporation of Cr and Y on the wear performance of TiAlN coatings at elevated temperatures // *Surf. Coat. Technol.* 1999, v. 115, p. 17-23.
13. L.A. Donohue, I.J. Smith, W.-D. Munz, I. Petrov, J.E. Greene. Microstructure and oxidation-resistance of  $Ti_{1-x-y-z}Al_xCr_yZr_n$  layers grown by combined steered-arc/unbalanced-magnetron-sputter deposition // *Surf. Coat. Technol.* 1997, v. 94-95, p. 226-231.
14. J.C. Sánchez-López, A. Contreras, S. Domínguez-Meister, A. García-Luis, M. Brizuela. Tribological behaviour at high temperature of hard CrAlN coatings doped with Y or Zr // *Thin Solid Films*. 2014, v. 550, p. 413-420.
15. J. Pelletier, A. Anders. Plasma-based ion implantation and deposition: A review of physics, technology, and applications // *IEEE Transactions on Plasma Science*. 2005, v. 33, LBNL-57610.
16. J. Musil, H. Hruby. Superhard nanocomposite  $Ti_{1-x}Al_xN$  films prepared by magnetron sputtering // *Thin Solid Films*. 2000, v. 365, p. 104-109.
17. S. Lee, S.-C. Wang, J.-S. Chen, J.-L. Huang. Effects of nitrogen partial pressure on electrical properties and thermal stability of TiAlN films by ion beam sputter deposition // *Surf. Coat. Technol.* 2007, v. 202, p. 977-981.
18. Z. Yujuan, Yan Pengxun, Wu Zhiguo, and Z. Pingyu. Influences of deposition parameters on the microstructure and properties of nanostructural TiN films synthesized by filtered cathodic arc plasma // *Rare Metals*. 2005, v. 24, p. 370-375.

19. V. Belous. Role of argon in the mixture with nitrogen at fabrication the condensates of Ti-Si-N system in the vacuum-arc deposition processes // *Zhurnal Tekhnicheskoi Fiziki*. 2013, v. 83(7), p. 69-76 (in Russian).
20. V.A. Belous, V.V. Vasylyev, V.S. Goltvyanytsya, S.K. Goltvyanytsya, A.A. Luchaninov, E.N. Reshetnyak, V.E. Strel'nitskij, G.N. Tolmacheva, O. Danylina. Structure and properties of Ti-Al-Y-N coatings deposited from filtered vacuum-arc plasma // *Surf. Coat. Technol.* 2011, v. 206, p. 1720-1726.
21. V. Belous, V. Vasylyev, A. Luchaninov, V. Marinin, E. Reshetnyak, V. Strel'nitskij, S. Goltvyanytsya, V. Goltvyanytsya. Cavitation and abrasion resistance of Ti-Al-Y-N coatings prepared by the PIII&D technique from filtered vacuum-arc plasma // *Surf. Coat. Technol.* 2013, v. 223, p. 68-74.
22. V.V. Vasylyev, A.A. Luchaninov, V.E. Strel'nitskij. High-productive source of the cathodic vacuum-arc plasma with the rectilinear filter // *Problems of Atomic Science and Technology*. 2014, v. 89(1), p. 97-100.
23. E.N. Reshetnyak. Features of using the X-ray fluorescence analysis for determine the composition of vacuum-arc nitride coatings // *Phys. Surf. Eng.* 2013, v. 11(4), p. 318-325.
24. A. Flink, T. Larsson, J. Sjolen, L. Karlsson, L. Hultman. Influence of Si on the microstructure of arc evaporated (Ti, Si)N thin films; evidence for cubic solid solutions and their thermal stability // *Surf. Coat. Technol.* 2005, v. 200, p. 1535-1542.
25. C.L. Chang, C.T. Lin, P.C. Tsai, W.Y. Ho, D.Y. Wang. Influence of bias voltages on the structure and wear properties of TiSiN coating synthesized by cathodic arc plasma evaporation // *Thin Solid Films*. 2008, v. 516, p. 5324-5329.
26. O.V. Sobol. On possibilities of control the phase composition, structure and stress in the vacuum-arc nanocrystalline coatings of the Mo-N system by adjusting the substrate bias potential during deposition // *Pis'ma v Zhurnal Tekhnicheskoi Fiziki*. 2012, v. 38(4), p. 26-33 (in Russian).
27. H.G. Feller, Y. Kharrazi. Cavitation erosion of metals and alloys // *Wear*. 1984, v. 93, p. 249-260.
28. Alicja K. Krella. Cavitation erosion resistance parameter of hard CAVD coatings // *Progress in Organic Coatings*. 2011, v. 70, p. 318-325.
29. A. Krella, A. Czyzniewski. Influence of the substrate hardness on the cavitation erosion resistance of TiN coating // *Wear*. 2007, v. 263, p. 395-401.
30. Alicja K. Krella. Cavitation erosion resistance of Ti/TiN multilayer coatings // *Surf. Coat. Technol.* 2013, v. 228, p. 115-123.
31. V.K. Pecharsky, P.Y. Zavalij. *Fundamentals of Powder Diffraction and Structural Characterization of Materials*. 2009, p. 744.
32. S. Mukherjee, F. Prokert, E. Richter, W. Moller. Intrinsic stress and preferred orientation in TiN coatings deposited on Al using plasma immersion ion implantation assisted deposition // *Thin Solid Films*. 2003, v. 445, p. 48-53.
33. C. Gautier, J. Machet. Study of the growth mechanisms of chromium nitride films deposited by vacuum arc evaporation // *Thin Solid Films*. 1997, v. 295, p. 43-52.
34. P.H. Mayrhofer, C. Mitterer, L. Hultman, H. Clemens. Microstructural design of hard coatings // *Progress in Mater. Science*. 2006, v. 51, p. 1032-1114.
35. D. Manova, J.W. Gerlach, S. Mändl. Thin film deposition using energetic ions // *Materials*. 2010, v. 3, p. 4109-4141.

Статья поступила в редакцию 22.01.2015 г.

## ИЗНОСОСТОЙКОСТЬ МНОГОКОМПОНЕНТНЫХ НИТРИДНЫХ ПОКРЫТИЙ НА ОСНОВЕ TiN И (Ti, Al)N, ОСАЖДЕННЫХ МЕТОДОМ PIII&D

**В.В. Васильев, В.С. Голтвяница, С.К. Голтвяница, А.А. Лучанинов, В.Г. Маринин, Е.Н. Решетняк,  
В.Е. Стрельницкий, Г.Н. Толмачева**

Многокомпонентные нитридные покрытия на основе TiN и (Ti, Al)N с малыми добавками Y, Re, Ni, Cr, Si, Mo, Fe синтезированы PIII&D-методом из фильтрованной катодно-дуговой плазмы. Во всех исследованных покрытиях обнаружена кристаллическая нитридная фаза с кубической структурой типа NaCl. Покрытия характеризуются твердостью 23...36 ГПа и модулем Юнга 324...436 ГПа. Добавка примесных элементов приводит к уменьшению средней скорости кавитационного и абразивного износа покрытий. Наилучшую стойкость и термостабильность показало покрытие, осажденное из катода состава  $Ti_{0.49}Al_{0.50}Y_{0.006}Re_{0.0005}$ .

## ІЗНОСОСТІЙКІСТЬ БАГАТОКОМПОНЕНТНИХ НІТРИДНИХ ПОКРИТТІВ НА ОСНОВІ TiN ТА (Ti, Al)N, ОСАДЖЕНИХ МЕТОДОМ PIII&D

**В.В. Васильєв, В.С. Голтв'яниця, С.К. Голтв'яниця, О.А. Лучанінов, В.Г. Маринін, О.М. Решетняк,  
В.Є. Стрельницький, Г.М. Толмачова**

Багатокомпонентні нітридні покриття на основі TiN й (Ti, Al)N з малими домішками Y, Re, Ni, Cr, Si, Mo, Fe синтезовані PIII&D-методом з фільтрованої катодно-дугової плазми. У всіх досліджених покриттях виявлено кристалічну нітридну фазу з кубічною структурою типу NaCl. Покриття характеризуються твердістю 23...36 ГПа та модулем Юнга 324...436 ГПа. Додавання домішкових елементів призводить до зменшення середньої швидкості кавітаційного та абразивного зносу покриттів. Найліпшу стійкість та термостабільність має покриття, осажене з катода складу  $Ti_{0.49}Al_{0.50}Y_{0.006}Re_{0.0005}$ .